19.[36] The conformations with one alkyl group *outside* are expected to be higher in energy. Structure **18** is more stable than **19**, because the *inside* position is less crowded sterically than the *anti* position. This leads to the observed anti-Cram stereoselectivity.[28,37] These results also support the notion that in protic solvents, the conformational preferences of the ketyl dictate the stereochemistry of dissolving metal reduction.

(36) Kagan et al. also suggested that SmI_2 reductions are most likely mediated by ketyl radical anions: Kagan, H. B.; Namy, J. L.; Girard, P. *Tetrahedron* **1981**, *37*, W175.

(37) Cram, D. J.; Elhafez, F. A. A. *J. Am. Chem. Soc.* **1952**, *74*, 5828. Cherest, M.; Felkin, H.; Prudent, N. *Tetrahedron Lett.* **1968**, 2199. Zioudrou, C.; M-Mavrides, I.; Chrysochon, P.; Karabatsos, G. T. *Tetrahedron* **1978**, *34*, 3181. Anh, N. T.; Eisenstein, O. *Nouv. J. Chem.* **1977**, *1*, 61. Lodge, E. P.; Heathcock, C. H. *J. Am. Chem. Soc.* **1987**, *109*, 3353.

Acknowledgment. We are grateful to Sir Derek H. R. Barton (Texas A&M University) for directing our attention to this interesting problem, to Dean Peter Rabideau (Louisiana State University) and Professor Paul von Rague Schleyer (University of Erlangen-Nurnberg) for helpful advice and extensive discussions, and to the National Institutes of Health for financial support of this research. We also thank the IBM Corp. for a grant of computer time on the IBM 3090/600J Supercomputer administered through the Office of Academic Computing at UCLA.

Layer-by-Layer Etching of Two-Dimensional Metal Chalcogenides with the Atomic Force Microscope

Ed Delawski[†] and B. A. Parkinson*[,‡]

Contribution from the Central Research and Development Department, The DuPont Company, P.O. Box 80328-216, Wilmington, Delaware 19880-0328, and Department of Chemistry, Colorado State University, Fort Collins, Colorado 80523. *Received September 3, 1991*

Abstract: The atomic force microscope (AFM) is used to etch off individual layers from the surface of two-dimensional metal dichalcogenide crystals, extending our earlier work on this phenomena with the scanning tunneling microscope (*J. Am. Chem. Soc.* **1990**, *112*, 7498). The etching proceeds via a nucleation and growth of holes, where the nucleation sites are provided by missing chalcogenide atoms from the surface of the crystal. Some substrates, such as $NbSe_2$, show faceted triangular etch pits which are observed to be rotated 180° on alternate layers, indicative of the polytype of the material. Counting nucleation sites over a given area provides a new method for determining extremely small deviations from stoichiometry in layered materials. The rate of the etching process was proportional to the force applied to the AFM tip. The mechanism for etching appears to be related to direct bonding interactions between tip atoms and substrate atoms with dangling bonds. The etching process could be simulated with a computer model relating the probability of removal of a given atom with its nearest neighbor environment. The implications of the strong interactions between AFM and STM tips and substrates probed in air are discussed. The nanofabrication of several small device-like structures is demonstrated.

Introduction

The scanning tunneling and atomic force microscopes have evolved into useful tools for the characterization and manipulation of matter on an extremely small scale. Probing surfaces in air with these techniques sets them apart from many other surface characterization techniques which require high vacuum conditions. Surfaces exposed to ambient conditions are always covered by adsorbed layers of water and hydrocarbon contaminants which can wet either an STM or AFM tip and, due to capillary forces, have a significant effect on the interaction between the tip and the substrate. Herein we extend our earlier work[1] on the layer-by-layer STM etching of 2D substrates, such as $SnSe_2$ and $NbSe_2$, to the AFM. The AFM has the advantage of allowing measurement and some control of the force applied to the tip facilitating the investigation of the role of the tip–substrate interaction in the etching process. Similar etching patterns and rates are obtained with the AFM, suggesting that the mechanism for removal of material is the same for both the STM and AFM. Our results perhaps shed some light on the controversy about the magnitude of tip interactions with the substrate during STM experiments performed in air.

Results

Figure 1 shows a series of AFM images taken by continuously scanning a 0.5 × 0.5 μm area of a $SnSe_2$ crystal with the AFM tip. The figure shows the nucleation and growth of rounded holes in the top layer of material resulting in the nearly complete removal of this layer and subsequent nucleation of the second layer. Continued scanning would result in the removal of many additional layers. The process is completely analogous to that observed on the same substrate with an STM tip.[1a] $NbSe_2$[1a] and MoS_2,[1b] when etched with the STM, produced triangular nucleation sites which continued to grow as triangular features and showed rotation of the triangle upon etching of the second layer. Figure 2 shows an analogous behavior with the AFM for $NbSe_2$. Note the 180° rotation of the triangles in the second layer due to the 2H polytype of the $NbSe_2$ where alternate layers are rotated 180° with respect to each other. The etched structures are completely stable over periods of several days exposure to laboratory air if they are not scanned by the AFM tip. Other layered structure dichalcogenides were also observed to etch in the AFM including TaS_2, SnS_2, $ZrSe_2$, $MoSe_2$, $HfSe_2$, and $TiSe_2$. $MoTe_2$, WSe_2, WTe_2, $ReSe_2$, and WS_2 crystals, grown in our lab, were not observed to etch. Graphite was also not observed to etch, but high forces did produce wrinkling of the graphite surface.

Variation of the force applied to the cantilever, via the piezoelectric elements of the AFM, resulted in the observation that the rate of removal of material was directly related to the applied force. Cratering, or buildup of material on the sides of the etched areas, was only observed at very high applied forces (>150 nN)

[†] The DuPont Company.
[‡] Colorado State University.

(1) (a) Parkinson, B. A. *J. Am. Chem. Soc.* **1990**, *112*, 7498-7502. (b) Parkinson, B. A. *Advances in Chemistry Series*; Bein, T., Ed.; in press.

0002-7863/92/1514-1661$03.00/0

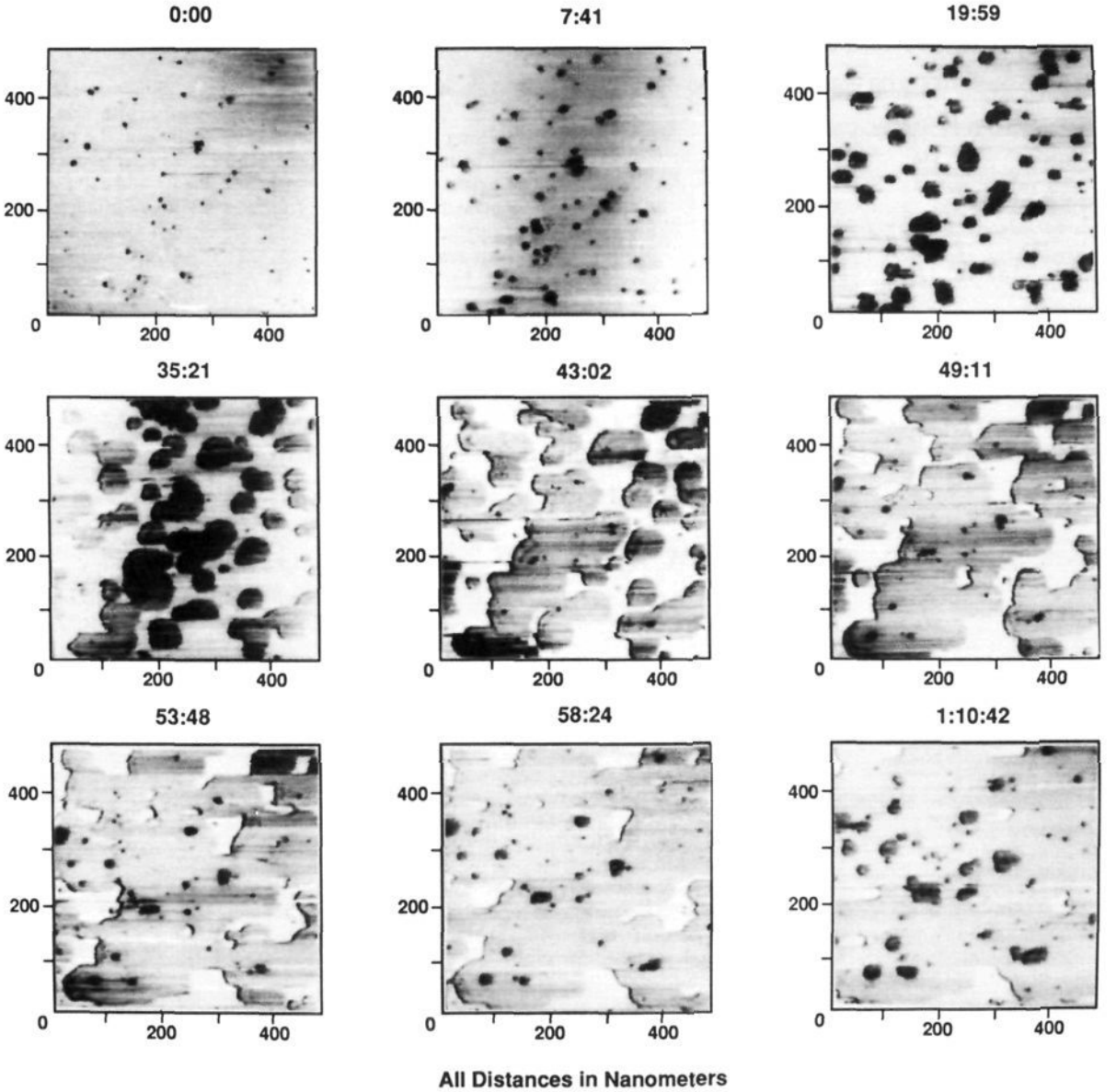

Figure 1. A sequence of 9 AFM images at different elapsed times (shown above each image) for the removal of a layer of $SnSe_2$ and beginning of second layer removal. The force was 80 ± 20 nN.

on $SnSe_2$. On $NbSe_2$ a force of 100 nN produced fast etching, but no cratering was observed. Higher applied forces did not produce etching in materials listed above which show no etching. Forces lower than 5 nN are difficult to study due to drifts in the apparatus over the long times needed to remove a layer at such low applied forces; however, reduction of the applied force to these low levels was useful for imaging structures without quickly expanding them.

A series of images saved at various times from the commencement of scanning over 0.5 μm areas (such as in Figures 1 and 2) were analyzed to determine the etched area and to measure the perimeter of the etched area. Etched area and etched area perimenter vs time curves for $NbSe_2$, shown in Figure 3, were obtained for four applied forces. If the inverse of either etching half-time, the time of maximum etch rate (first derivative = 0 for curves in Figure 3) or the time of maximum perimeter, is plotted vs the applied force a linear relationship is revealed as shown in Figure 4. During periods of rapid etching, associated with large exposed perimeter, doubling and even tripling of the image was often observed making stored images unusable for image processing.

The nucleation density can vary considerably from sample to sample as can be seen by comparing Figures 1 and 2. We associate nucleation sites with missing atom defects in the van der Waals surface of the material. High quality crystals of SnS_2, grown with excess sulfur in the Bridgeman ampules, resulted in substrates which did not etch, presumably due to lowering the number of sulfur vacancies in the material. A small dose of 5 keV Kr ions was impinged onto the surface of such an SnS_2 sample. When this sample was scanned by the AFM tip, easy removal of the top layer of material resulted, but subsequent layers were not observed to etch. This experiment suggests a new method for probing the damage depth associated with different energy, mass, and angle of ions impinging on a surface in ion sputtering experiments.

The relative humidity of the ambient air was also observed to affect the etching rate of the substrate. In one set of experiments a $NbSe_2$ sample was scanned with a force of 45–55 nN in 100% relative humidity (a beaker of hot water enclosed within the AFM chamber), 70% (ambient laboratory air) relative humidity, and with several desicants (Drierite and activated Linde 4 Å molecular sieves resulting in <30% relative humidity) inside the acoustic isolation dome covering the AFM head. The etching rate at nearly constant applied force was observed to increase with the relative humidity. The force distance curves shown in Figure 5 reflect the increase in capillary forces on the cantilever/tip when an absorbed water layer is present on the surface. Figure 5c shows

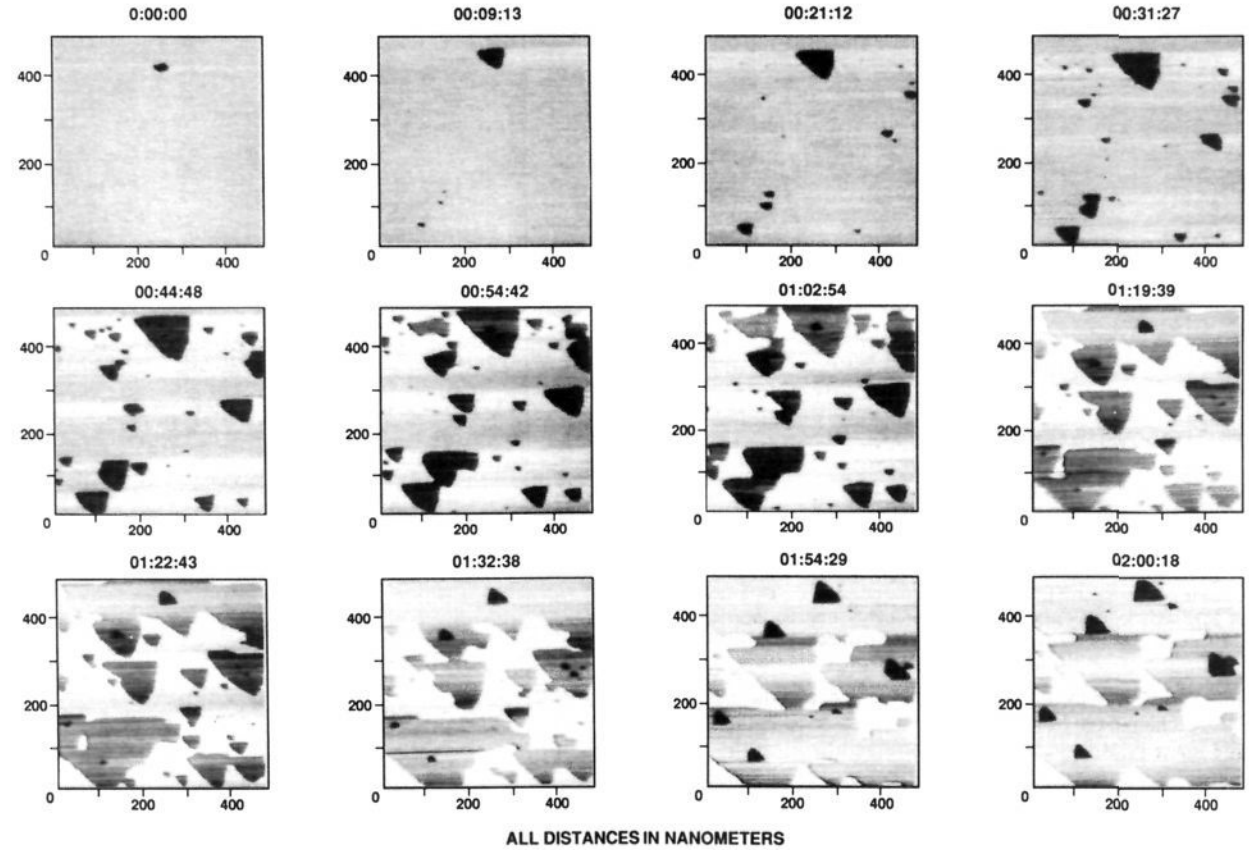

Figure 2. A sequence of 12 AFM images at different elapsed times for the removal of a layer of $NbSe_2$ and subsequent nucleation and initial removal of a second layer. Note the rotation of the triangular holes in the subsequent layer. The force was 19 ± 5 nN.

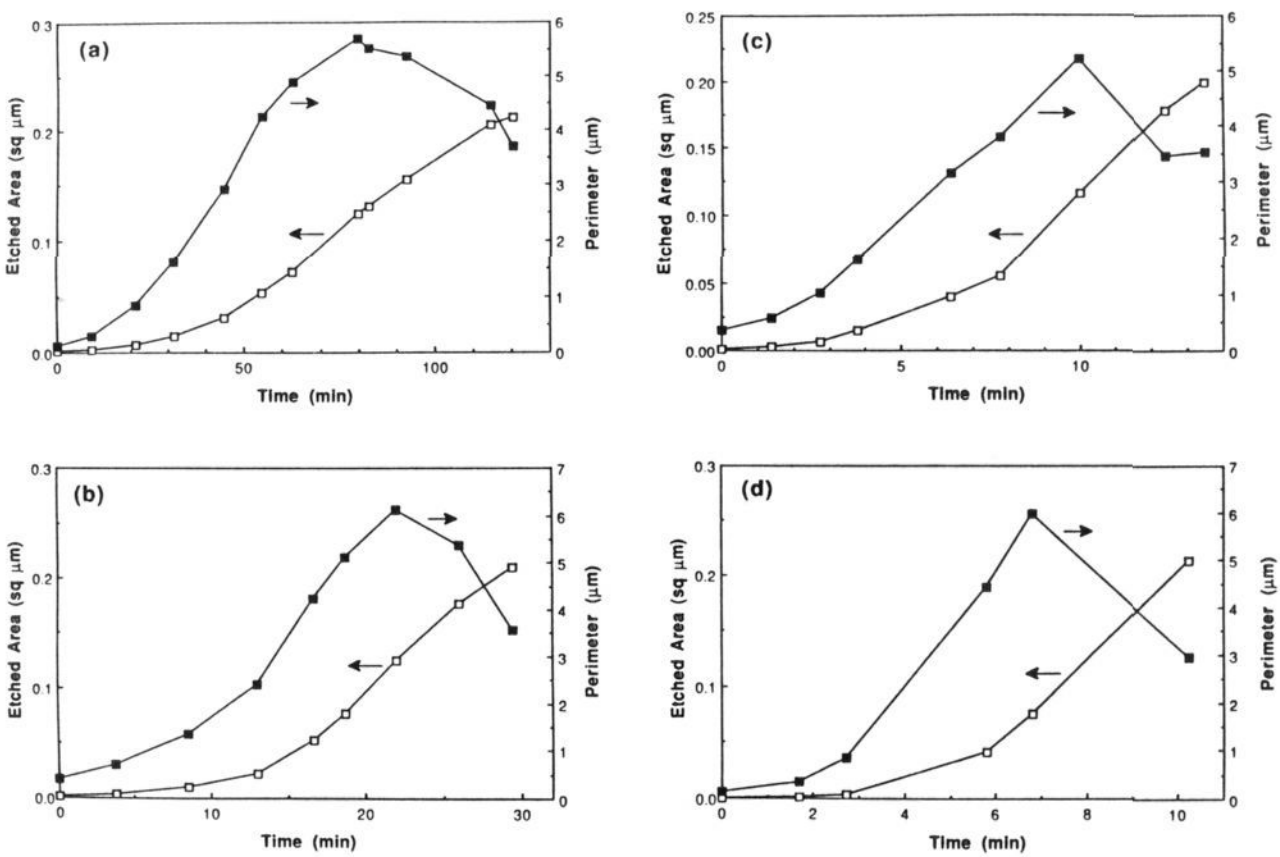

Figure 3. A series of curves showing etched area (open symbols, left axis) and exposed perimeter (closed symbols and right axis) for removal of a layer of $NbSe_2$ at various applied forces. The applied forces were 18, 37, 63, and 96 nN for a–d, respectively.

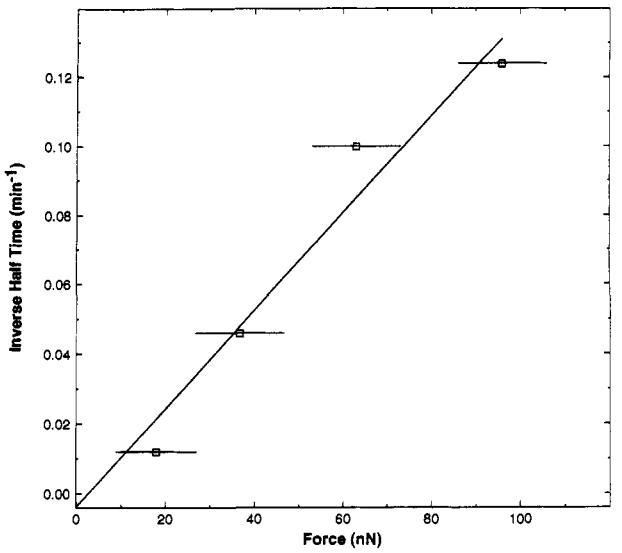

Figure 4. Inverse of the time to remove half a 0.5 × 0.5 μm of $NbSe_2$ layer (from Figure 3) plotted against the applied force in nanonewtons. The line is a least-squares fit also including the origin in the data set. The error bars include uncertainties in determining the applied force as well as drift in the force over the course of an experiment.

a large hysteresis in the approach-release curve due to the presence of the high humidity. Much less hysteresis is observed in the curves at the lower relative humidities (Figure 5a,b).

Mechanism and Computer Model

The importance of preexisting nucleation sites, which grow into macroscopic holes, suggests that the mechanism of material removal involves surface atoms with unsaturated coordination. The interaction of the tip with the sample preferentially removes these unsaturated atoms. A simple intuitive model would predict easier removal of atoms with fewer nearest neighbors than atoms with many nearest neighbors (nn). A computer program was written to simulate a hexagonal lattice allowing a predetermined number of nucleation sites and variation of a series of probabilities for removal of atoms with a given number of nearest neighbors (zero to six). The program then sequentially interrogates every atom position deciding whether or not an atom should be removed from the lattice and repeats the process until all the atoms are removed. A number of significant simplifications such as reducing a three atom layer to a single atom layer and ignoring the special directions in the lattice determined by the metal site occupancy are implicit in the model. Nonetheless simulated etching pictures look remarkably like the real data if the probability of six nearest neighbor removal is set to zero (no new nucleation) and the probabilities of atom removal are in the order 5 nn < 4 nn < 3 nn < 2 nn ≤ 1 nn ≤ 0 nn (probabilities for removal of 0 and 1 nn atoms is often set to 1.0). Figure 6 shows a series of computer generated pictures of etching of a 200 × 200 hexagonal array of atoms with atom probabilities showing a geometric sequence (see figure caption). The number of nuclei was set to 120 to be similar to the $SnSe_2$ sequence shown in Figure 1. The distance scale of Figure 1 is about seven times the number in Figure 6, but we assume the process scales over this relative distance.

Figure 7 shows a comparison of the etched area vs time curves for the computer model and the curve from analysis of Figure 1. A relatively good fit is obtained from an arbitrary normalization of the time axis with time axis with iterations from the computer simulation. We do not intend to present this model as a unique solution to the etching mechanism but rather as a very simple intuitive model which does a reasonable job of reproducing the real data. Indeed many mechanisms could be envisioned to remove atoms with such relative probabilities. In light of this an exhaustive optimization of the fit of the real and simulated curves by manipulation of the six adjustable probabilities was not done. However the general trend of 5 nn atoms being very difficult to

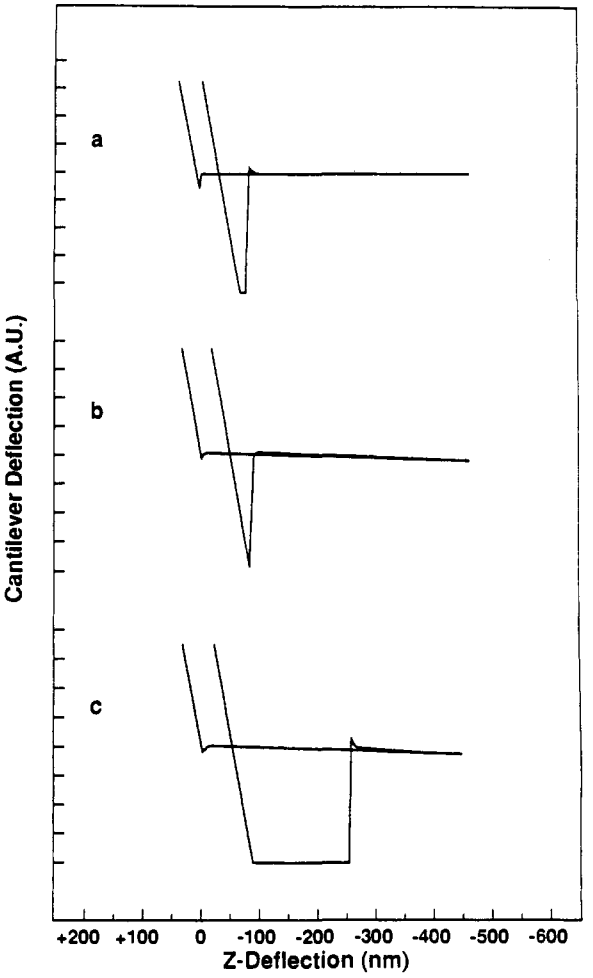

Figure 5. Typical approach-release curves for an $NbSe_2$ surface for (a) dry (<30% humidily) conditions, (b) normal laboratory air (70% relative humidity), and (c) 100% relative humidity air (beaker of steaming water set inside AFM cover).

remove with respect to other nn environments was necessary to produce simulations showing the delayed appearance of nucleation sites that was observed in the real system. The same effect could be simulated by addition of a very small new nucleation probability, but this was not justified from our experiments on the non-nucleating (and thus nonetching) crystals.

Faceting, to produce triangular and rhombic features as was observed on some substrates, can also be introduced in the computer model by artificially stabilizing a 4-nn site over a 5-nn site. The origin of the triangular features in Figure 2 is most probably related to the presence of special crystallographic directions due to the metal atoms in every other trigonal prismatic site between the chalcogenide layers, and this further complexity was not added to the computer model. Dendritic and fingered growth can also be simulated with the program by adjustment of the nn removal probabilities, but these morphologies were not observed in our AFM of STM etching experiments.

Discussion of Mechanisms

The similarity of the number and shape of nucleation sites and the rates of removal of material when etching 2D materials with either an STM or an AFM suggests a similar mechanism in both cases. Mechanisms related to the continuous current flow such as carrier relaxation and resistive heating of the surface, which were previously postulated as mechanisms for STM etching,[1a] can clearly be eliminated by the AFM results presented herein. Electrochemical reactions related to the bias difference between the STM tunneling tip and the substrate are also unlikely, but local open circuit corrosion reactions, where, for instance, the tip material or adsorbed impurity is oxidized and substrate material is reduced, are still possible. However we feel this is unlikely due

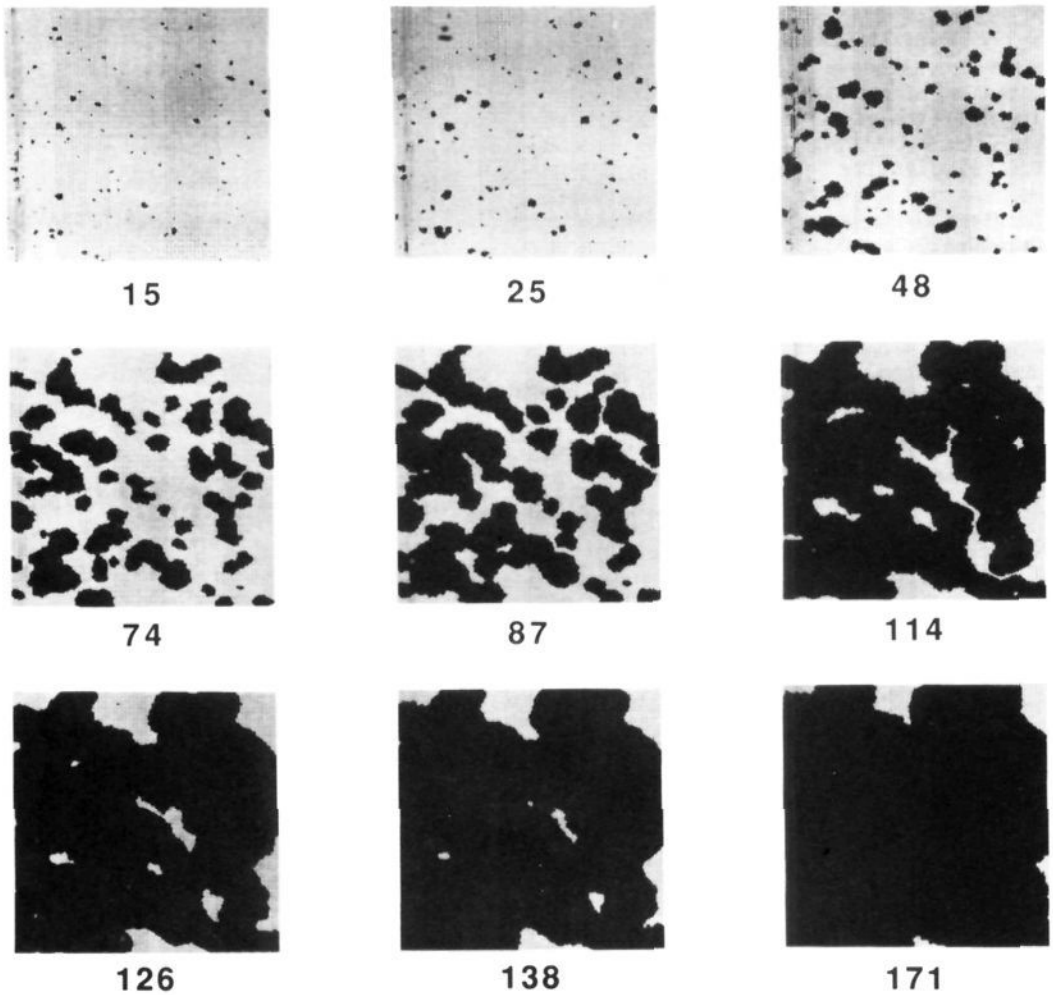

Figure 6. Simulated etching sequence for $SnSe_2$ type etching substrate. The numbers above each frame represent the interaction number with the frames chosen to compare with Figure 1.

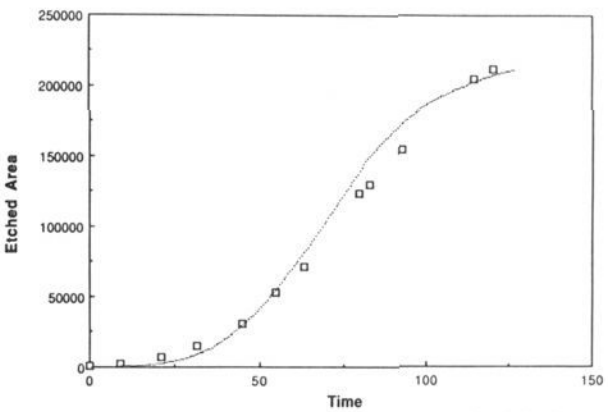

Figure 7. Etched area vs time curves for the computer simulation (small points) and for the etching of $SnSe_2$ by the AFM (square symbols). Data are from Figure 1.

to the Si_3N_4 AFM tips which are quite inert to oxidation or reduction.

Field ionization processes also seem unlikely since the field between the tip and sample in the AFM experiment, due to the contact of different work function materials, is probably much less than the field applied to an STM tip. Also, if the field was important for the etching process we would expect substantial differences in etching rates between metal and semiconducting substrates due to the penetration of the field (space charge layer) into the semiconductors, reducing its magnitude at the surface. For example some metallic substrates were observed to etch (i.e., TaS_2) and some not (i.e., WTe_2), and some semiconductor substrates were observed to etch (i.e., SnS_2) and some not (i.e., $MoTe_2$).

A physical interaction between the AFM (STM) tip and the substrate now seems to be the most likely mechanism for removal of material from the surface of the layered compound substrates. One could imagine at least two different interaction mechanisms which we will term local and nonlocal. The nonlocal mechanism involves energy dissipation from frictional forces arising from scanning the tip over the surface. Local heating or compression of the substrate may excite phonons which scatter inelastically from the defect sites and unsaturated atoms and provide enough energy to thermally evaporate atoms. Theoretical calculations may provide further insight into the plausibility of this mechanism.

The local mechanism is simply bonding of dangling bonds at edge sites directly to the tip material with sufficient strength to remove them from the lattice. The nearest neighbor probabilities for atom removal, which reproduce the etching patterns in the computer model, follow naturally from this simple model. An atom which can form two or more bonds with the tip is more likely to be removed. The removal of edge site atoms would also be facilitated by the lateral forces due to the tip interacting with the steps. Meyer and Amer[2] used an instrument with cantilevers similar to those used by us, but capable of measuring both bending and torsional deflections when traversing steps on a NaCl crystal. They estimate the excess energy on traversing a 2.8-Å step is on the order of 50 eV. Since the step heights on the materials discussed herein are all greater than 6 Å, higher excess energy would be expected. Additional evidence for the direct lateral interaction of the tip with the steps can be seen by careful ex-

amination of Figure 2. In Figure 2 we observed that a triangular edge, forming a small angle with respect to the scan direction, tends to have that edge etched to be parallel to the scan direction. This can be explained by the higher lateral force applied to this edge due to trapping of the tip in the etch pit. Rotation of the scan direction again results in any edge forming a small angle with the scan direction eventually being aligned to it. STM etching of MoS_2 crystals resulted in very slow formation of almost perfect equilateral triangular etch pits,[1b] also observed for STM etching of $NbSe_2$,[1a] suggesting the lateral forces are not as important in the case of STM where the tip is farther from the surface.

The minimum interaction time for a tip atom and a given substrate atom can be calculated (from the maximum scan rate, maximum scan size, and the size of an atom) to be greater than 1 μs. Bond-forming and -breaking processes are considered to be on a much shorter time scale, suggesting there is time for the substrate atoms to form bonds with the tip atoms.

$SnSe_2$ samples which could be etched in air were not observed to etch with an STM operating in ultrahigh vacuum presumably due to the true tunneling gap preventing mechanical interaction between tip and substrate.[3] This result, when taken with the AFM results in various relative humidity atmospheres, suggests that the adsorbed water layer, found on most materials when exposed to humid air, plays a role in the etching process. Capillary forces, as a result of wetting the AFM/STM probe when it contacts the surface, would contribute to the force between the probe and the substrate. Capillary forces between a sphere and a surface due to a liquid bridge can be calculated, assuming a radius of curvature for the AFM tip of 10 nm, to be less than 10 nN.[4] Etching rates observed on $NbSe_2$ with a force of 7.9 nN are similar to those observed in STM etching experiments on this substrate suggesting that the capillary forces on an STM tip are enough to facilitate etching. Other workers have studied the interaction of STM and AFM tips with substrates in air and have reached similar conclusions about the order of magnitude of the forces involved and the influence of contamination layers.[5-14]

Water could also act as a weakly bound ligand for unsaturated bonds at an edge site atom which can be displaced by atoms on the probe tip. AFM etching experiments on $SnSe_2$ crystals conducted under bulk water also showed etching behavior with a rate similar to that observed in air. AFM etching experiments in UHV, where the force can be varied while the tip is in contact with surface with no adsorbed layers present, will be most useful in elucidating further details of the etching mechanism. It is also possible that several of the mechanisms described above are operating synergistically to enable the controlled removal of material.

The doubling and tripling of the image during rapid etching can be attributed to accumulation of material on the tip. The periods of maximum etch rate are often associated with the coalescence of pits often leaving small isolated islands of material. When the bonding strength of edge atoms on these islands to the tip exceeds the weak van der Waals attraction of the island to the layer below, the entire small island would be picked up by the tip resulting in multiple tip effects (since the van der Waals forces may be a thousand times weaker than the covalent bonds within a layer, it is easy to see how an island of several hundred atoms could be removed). Often these multiple tip effects disappear after several additional scans suggesting that the material, due to capillary forces, is able to migrate up the tip. We seldom see extra material on the surface adjacent to the etched areas when a larger area around an etched feature is scanned.

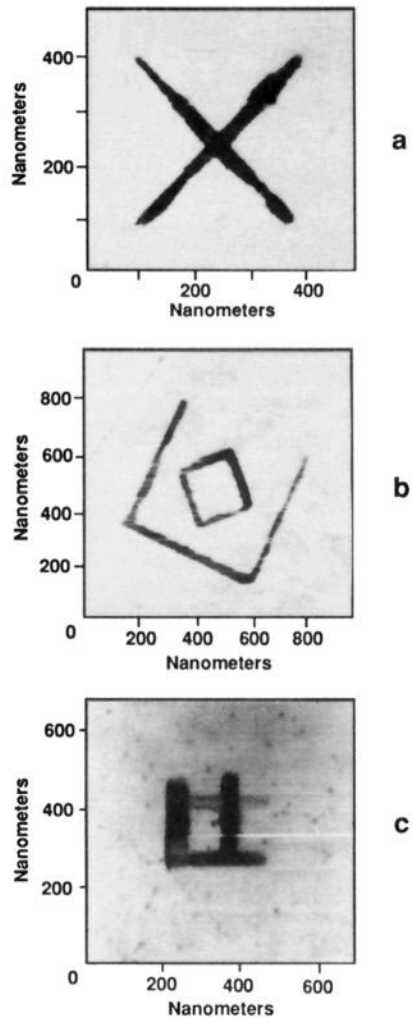

Figure 8. Several etched structures which were created by disabling one scan axis and moving and rotating the scan. See text for significance of various features.

The materials property which separates the materials that are observed to etch from those that do not is not obvious. In general highly covalent materials such as $MoTe_2$, WTe_2, and $ReSe_2$ (the latter two contain metal–metal bonds) do not etch, whereas the most ionic materials (SnS_2, $TiSe_2$, and $ZrSe_2$) etch readily. The presence of missing atom sites, necessary for the nucleation of the etching process, may be related to the covalency of the material and the materials ability to compensate the missing charge. The thermodynamics of the formation of the missing chalcogenide sites under conditions we use for crystal growth may promote nonstoichiometry in the more ionic materials. Why $MoSe_2$ was often observed to etch and WSe_2 was not, even though the crystal growth method and physical properties of these two materials are very similar, must be related to the presence of defects in the former material. Recently WSe_2 was observed to grow triangular pits after repeated scanning of an area purposely damaged via a 10–400 ns 5 V voltage pulse.[15]

(2) Meyer, G.; Armer, N. M. *Appl. Phys. Lett.* **1990**, *57*, 2089–2091.
(3) Lieber, C. Private Communication, 1990.
(4) Israelachvili, J. N. *Intermolecular and Surface Forces*; Academic Press: 1985; pp 221–226.
(5) Salmeron, M.; Ogletree, D. F.; Ocal, C.; Wang, H-C.; Neubauer, G.; Kolbe, W.; Meyers, G. *J. Vac. Sci. Technol. B* **1991**, *9*, 1347.
(6) Durig, U.; Gimzewski, J. K.; Pohl, D. W. *Phys. Rev. Lett.* **1986**, *57*, 2403.
(7) Yamada, H.; Fujii, T.; Nakayama, K. *J. Vac. Sci. Tech. A* **1988**, *6*, 293.
(8) Hartmann, U. *Adv. Mater.* **1990**, *2*, 594.
(9) Weisenhorn, A. L.; Hansma, P. K.; Albrecht, T. R.; Quate, C. F. *Appl. Phys. Lett.* **1989**, *54*, 2651–2653.
(10) Van Labeke, D.; Labani, B.; Girard, C. *Chem. Phys. Lett.* **1989**, *162*, 399–403.
(11) Gould, S. A. C.; Burke, K.; Hansma, P. K. *Phys. Rev. B.* **1989**, *40*, 5363–5366.
(12) Tang, S. L.; Bokor, J.; Storz, R. H. *Appl. Phys. Lett.* **1988**, *52*, 188–190.
(13) Blackman, G. S.; Mate, C. M.; Philpott, M. R. *Phys. Rev. Lett.* **1990**, *65*, 2270–2273.
(14) Meepagala, S. C.; Real, F.; Reyes, C. B. *J. Vac. Sci. Technol. B.* **1991**, *9*, 1340.
(15) Akari, S.; Möller, R.; Dransfeld, K. *Appl. Phys. Lett.* **1991**, *59*, 243.

The observed nucleation density may also provide a method of determining the small nonstoichiometry of the layered materials which etch. For instance the approximately 120 nucleation sites measured in the 0.5 × 0.5 μm area of Figure 1 results in a formula of $SnSe_{1.9999}$ for the material. The 40 nucleation sites observed in Figure 2 result in a formula of $NbSe_{1.99998}$. We do not know at this time whether missing chalcogenide atoms on the bottom of a layer or missing metal atom sites are active as nucleation sites for etching. Small deviations from stoichiometry such as this are difficult to determine by direct analytical methods. The amplification provided by the growth of the nuclei could in principal make this method sensitive to greater than 1 part of the 10^8 for the direct measurement of nonstoichiometry. An earlier technique, used to magnify defects on graphite[16] and MoS_2,[17] used a thermal treatment in oxygen at high temperatures to grow pits. In the case of MoS_2 triangular structures could be seen with interference microscopy after oxidation and decoration with evaporated Au. The triangles also showed 180° rotations on successive layers.[17] The oxidation of graphite defects to produce hexagonal etch pits could also be followed via the STM.[16b]

Nanofabrication with the AFM

Figure 8 shows several structures which could be fabricated by custom rastering of the AFM tip. The 300 nm "X" in Figure 8a has lines which are only 20 nm wide and are one unit cell of $SnSe_2$ deep (0.6135 nm). This structure was created by disabling one of the scan axis of the microscope and then rotating the scan. The line width apparently is controlled by the thermal drift in the microscope during the time it takes to etch the line (less than 2 min) and perhaps the bluntness of the tip although these tips are routinely capable of atomic resolution on these substrates. Figure 8b shows the complexity that can be generated by careful control of raster size and direction. We call this feature the "ice cube in a glass".

Figure 8c illustrates a structure on a single material which is a useful model for etching tiny device structures when combined with the recently developed technique of van der Waals epitaxy. With this technique multilayer structures of various 2D materials can be built up with molecular beam epitaxy, without regard for lattice matching, due to the lack of interlayer covalent bonding.[18] In Figure 8c a single layer mesa of about 50 × 100 × 0.6 nm has been isolated from the surrounding material of the top layer but retains a connection with the second layer down. If the second layer was configured to be a conducting dichalcogenide such as $NbSe_2$ and the top was a semiconducting material, all deposited on an insulating substrate (third layer down), a very small diode structure would result which could be contacted with an STM tip. Construction of single quantum sized devices with these technologies would be of considerable research interest although any practical applications would require multiplexing of AFM and/or STM tips. Again we emphasize that these structures were completely stable upon exposure to laboratory air as long as they are not scanned by the AFM. Reducing the force applied to the AFM tip during scanning significantly reduced the continual etching of the fabricated structures.

Conclusions

We have demonstrated that the STM etching process we previously reported[1a,b] is nearly identical to etching observed with the AFM. We showed that the rate of this etching process is dependent on the force applied to the AFM tip and is related to the relative humidity. The similarity of the STM and AFM etching processes points out that substantial interaction forces between an STM tip and a substrate are present when operating in humid air. We ascribe the etching mechanism to a mechanical interaction between the AFM tip and the substrate resulting in bonding of unsaturated substrate atoms to the tip. A simple computer model, based on probabilities of removal of atoms with different nearest neighbor environments, was able to produce etching patterns much like those observed in real systems. Several small complex features were created demonstrating the utility of this technique for nanolithography.

Experimental Section

A Nanoscope II AFM from Digital Instruments, Santa Barbara, CA was used for all AFM imaging, etching, and step measurements. Imaging and etching was done in the constant-force mode with a scanning head having a 12 μm range at scan rates between 4.34 and 19.53 Hz for the 400 × 400 pixel image. The integral and proportional gains were between 1.84 and 3.25, respectively, and the 2D gain was between 0.00 and 0.04. Most of the etching experiments were done on 0.5 × 0.5 μm areas. Imaging under water was done in a liquid cell supplied by the manufacturer.

Si_3N_4 micromachined cantilevers (nanoprobes supplied by Digital Instruments) with a spring constant of 0.58 N/m were used. Force values were calculated according to the manufacture's specifications using the point at which the tip to sample force is attractive as our zero force reference.[19] The forces reported for extended etching times were the average of the force determined before and after the etching experiment. This is necessary due to unavoidable drift in the applied force with time.

Crystal samples were mounted on steel discs with cyanoacrylate adhesive and cleaved via sticky tape before each experiment. $SnSe_2$ and SnS_2 crystals were grown with a Bridgeman technique. All other materials were grown via chemical vapor transport reactions in sealed quartz ampules with only small variations of published procedures.[20]

Image analysis was done with a Macintosh IIci computer running a public domain software package called "IMAGE" developed at the NIH. The etching simulations were also done on a Macintosh IIci computer programmed with Z BASIC.

Acknowledgment. Greg Blackman was most helpful in the discussions of AFM tips/surface interactions. Scott McLean and Pat Morris helped in the crystal growth of substrates. Dennis Swartzfager provided the ion sputtering facilities, and Paul Meakin assisted our understanding of the fractal nature of the etching process.

Registry No. $SnSe_2$, 20770-09-6; $NbSe_2$, 12034-77-4; SnS_2, 1315-01-1; TaS_2, 12143-72-5; WTe_2, 12067-76-4; $MoTe_2$, 12058-20-7; $ZrSe_2$, 12166-47-1; $MoSe_2$, 12058-18-3; $HfSe_2$, 12162-21-9; $TiSe_2$, 12067-45-7; WSe_2, 12067-46-8; $ReSe_2$, 12038-64-1; WS_2, 12138-09-9.

(16) (a) Henning, G. R. *Chemistry and Physics of Carbon*; Walker, P. L., Ed.; Marcel Decker, Inc.: New York, 1966; Vol. 2, p 1. (b) Chang, H.; Bard, A. J. *J. Am. Chem. Soc.* **1990**, *112*, 4598.

(17) Bahl, O. P.; Evans, E. L.; Thomas, J. M. *Proc. Royal Soc. A* **1968**, *306*, 53–65.

(18) (a) Koma, A.; Yoshimura, K. *Surf. Sci.* **1986**, *174*, 556. (b) Ueno, K.; Saiki, K.; Shimada, T.; Koma, A. *J. Vac. Sci. Technol. A* **1990**, *8(1)*, 68. (c) Ohuchi, F. S.; Shimada, T.; Ueno, K.; Parkinson, B. A.; Koma, A. *J. Crystal Growth*. In press. (d) Ueno, K.; Koma, A,; Ohuchi, F. S.; Parkinson, B. A. *Appl. Phys. Lett.* **1991**, *58*, 472.

(19) Forces were calibrated using the point of initial tip to sample attraction as a reference for zero force and the formula

$$F = k\Delta V(dz/dV)$$

where k = spring constant of cantilever (0.58 N/m for 100 μm cantilever) ΔV = set point voltage applied − set point voltage for zero cantilever deflection, dz/dV = change in z-distance with respect to cantilever deflection voltage.

(20) Lieth, R. M. A. *Preparation and Crystal Growth of Materials with Layered Structure*; D. Reidel: Dordrect, 1977.